Hindawi
Advances in Polymer Technology
Volume 2020, Article ID 8794076, 10 pages
https://doi.org/10.1155/2020/8794076

Research Article

Experimental Study of Moisture Content Effect on Geotechnical Properties of Solidified Municipal Sludge

Yijun Chen,[1,2,3] **Xingxing He**,[1,4] **Ping Wang**,[1,2,3] **Yong Wan**,[1,2,3] **and Xun Tan**[1,4]

[1]*State Key Laboratory of Geomechanics and Geotechnical Engineering, Institute of Rock and Soil Mechanics, Chinese Academy of Sciences, Wuhan 430071, China*
[2]*IRSM-CAS/HK PolyU Joint Laboratory on Solid Waste Science, Wuhan 430071, China*
[3]*Hubei Province Key Laboratory of Contaminated Sludge & Soil Science and Engineering, Wuhan 430071, China*
[4]*University of Chinese Academy of Sciences, Beijing 100049, China*

Correspondence should be addressed to Yijun Chen; yjchen@mail.whrsm.ac.cn and Xingxing He; hexingxing16@mails.ucas.ac.cn

Received 4 August 2019; Revised 3 November 2019; Accepted 14 November 2019; Published 17 January 2020

Guest Editor: Zhang Zhien

Moisture content is an important factor affecting the geotechnical properties of solidified municipal sludge (MMS). Typical municipal sludge in China was chosen to investigate the effects of initial moisture content (defined as w_0) on geotechnical properties of MMS solidified by self-developed CERSM solidifying agent. In addition, the microstructure changes of solidified sludge samples in this study were explored with scanning electron microscopy and mercury intrusion porosimetry. Mechanical experiment results showed that the unconfined compressive strength, cohesion, and internal friction angle of the MMS increased with the decrease in initial moisture content, but the permeability coefficient changed oppositely. The permeability coefficient of solidified sludge samples was between 10^{-8} and 10^{-10} cm/s. But after the drying-saturated process, the permeability coefficient of MMS can be increased up to 4 times, mainly due to the formation of a considerable number of microconnected pores and microcracks in the process of drying. The research results are of great significance to the safe disposal and utilization of municipal sewage sludge in China.

1. Introduction

The output of municipal sewage sludge has risen dramatically with the continuous increase in municipal sewage production in China. The country's municipal sewage sludge output is expected to exceed 60 million tons by 2020. The huge amount of sludge will cause substantial environmental problems [1–3], and thus, sludge stock absorption through various disposal methods should be urgently considered. The municipal sludge is often solidified with materials and then used as landfill cover materials [4, 5], subgrade fillers [6], garden soil [7], and brick-making materials [8] or landfilled [9].

Some scholars have conducted theoretical and experimental studies on sludge solidification with different solidifying agent. Yang et al. [10] used coal gangue, cement, clay, and fiber to solidify municipal sewage sludge, and they found that the solidified sludge can be used as landfill cover materials with high strength, strong crack resistance, and low permeability coefficient characteristics. Vu et al. [11] solidified the sludge with fly ash geopolymer and found that the solidified sludge can reach the maximum compressive strength after 18 hours. The studies mostly focused on sludge with high moisture content [12, 13], however, only few research has been conducted on the influencing mechanism of different initial moisture contents on the geotechnical properties of the solidified sludge.

Research has shown that moisture content is an important index affecting a series of engineering properties, such as shear strength [14, 15], unconfined compressive strength [16, 17], and permeability coefficient [18, 19] of solidified sludge. Boutouil and Levacher [12] studied the influence of initial water content on the mechanical behaviour of solidified dredged sludge, and found that there was a good linear relationship between compressive strength and the inverse of water/cement ratio. Lin et al. [20] also found that an increase of the initial water content of the sewage sludge reduced the compressive strength of the solidified sludge largely. Horpibulsuk et al. [21] researched the compression behavior of solidified soft soil with different initial water content,

Table 1: Detection results of sludge XRF/%.

Elements	Mg	Al	Si	P	S	K
Content	3.195	14.355	39.345	4.85	7.165	3.54
Elements	Ca	Ti	Mn	Fe	Cu	Zn
Content	10.8	1.09	0.28	13.955	0.175	1.245

showing that the specimens with higher water content are stable at higher void ratios and provide higher compression indices beyond the transition stress. Wang et al. [22] investigated the shrinkage properties of cement solidified sludge influenced by the initial moisture content. But on the whole, the effect of initial moisture content on the permeability of solidified sludge is rarely studied, especially combined with microscopic analysis method. Most previous studies have addressed the issue of whether the solidified sludge meets landfill requirements. However, few people consider the solidified sludge as the impermeable layer material of landfill, which will be further explored in this study.

In this study, the sludge with different initial moisture contents was prepared and then solidified by the self-developed cement-based CERSM solidifying agent. Then, the shear strength, compressive strength, permeability coefficient, and other engineering characteristic parameters of the CERSM-solidified sludge with different initial moisture contents and drying-saturated (DS) condition were studied by conducting direct shear test (DST), unconfined compression test (UCT), and permeability test (PT). The microtopography of the solidified sludge pore structure was studied by scanning electron microscopy (SEM) and mercury intrusion porosimetry (MIP), and the relationship of the testing results with the engineering properties was analyzed. The research results can greatly support the modification and solidification of municipal sewage sludge and its utilization in China.

2. Materials and Methods

2.1. Test Materials. The sludge was collected from the Wuhan Sewage Treatment Plant in Hubei, China. The basic properties of the sludge were tested immediately after collection. The initial moisture content was 82.98%, the density was 1.14 kg/m^3, the pH value was 7.07, the organic matter content was 38%, and the COD was 2868 mg/L. The composition of the chemical elements in the sludge was tested with X-ray fluorescence. The results are shown in Table 1.

The CERSM solidifying agent used in the test was optimized by a previous research on sludge modification [23]. The solidifying agent was composed of a sulphoaluminate-based cement, ordinary Portland cement, quicklime, gypsum, and lithium salt, by which the corresponding mass ratio was 0.30 : 0.60 : 0.05 : 0.049 : 0.001. Calcium oxide accounted for 88.3% of the total weight of quicklime used in the test, and HCl dissolution content was less than 1%. More than 95% of the quicklime particles can pass through a 200-mesh sieve. The basic solidifying agent of sulphoaluminate cement (SAC) was labeled 42.5, the specific surface area was 430 m^2/kg, the initial setting time was more than 25 min, the final setting time was less than 180 min, the pH value of 1 h was less than 10.5, and the free swelling ratio of 28 d (curing age) was less than 0.15%. The ordinary Portland cement was labeled 42.5 and produced by the Huaxin Cement Plant of Wuhan city. The density of the CERSM solidifying agent was 1.83 kg/m^3, and the specific surface area of Blaine was 360 m^2/kg.

2.2. Test Method and Equipment

2.2.1. Preparation and Curing of Solidified Sludge Samples. Due to the moisture content of sludge from different sewage treatment plants in China varies from 50% to 85% [24], in this study, the sludge samples with target w_0 of 85%, 81%, 77%, 74%, 71%, 63%, and 56% were prepared and then labeled as Samples 1–7, just as shown in Table 2. The self-developed strong dehydration equipment for the sludge (Figure 1) was used to thoroughly dewater the sludge with moisture content of 80%. The dehydration process was conducted as follows. First, the moisture content of the sludge was adjusted to 90%, and a part of the free water with pressure of 0.8 MPa was dehydrated in the feeding process. Moisture content was dewatered to 70–80%. Then, the appropriate pressure was applied for the secondary extrusion to dehydrate the sludge to a certain moisture content (nearly 55%). Finally, the appropriate amount of water was calculated and added into the sludge for target moisture content adjustment.

The solidified sludge was obtained by adding the CERSM solidifying agent according to 20% wet weight of the sludge to the prepared sludge mentioned above (define Aw as the addition ratio of solidifying agent, and Aw = 20% in this study). The CERSM materials were weighed according to their design proportions and then placed in the mixer. Then, 2 min of slow stirring followed by 2 min of quick stirring were conducted to produce a homogenous mixture. The mixture was subsequently placed into an unconfined compression mold (Φ50 mm × 100 mm), a shear test mold (Φ61.8 mm × 20 mm), and a penetration test mold (Φ50 mm × 50 mm). The filling process was divided into three layers, and the filling in the last layer was 1 cm higher than the mold (or ring knife). Then, the mold filled with solidified sludge was placed on a shaking table to vibrate for 2 min and then shaved up and down with a scraper. Subsequently, the molded samples were wrapped with a plastic film and placed into a curing box at 20°C with relative humidity of 95% for standard curing. The solidified sludge samples were demolded after 1 day of standard curing. Finally, the solidified samples were sealed with a film to avoid the evaporation of moisture.

2.2.2. Drying-Saturated (DS) Treatment. After curing for 28 d, all the solidified samples were DS treated, and then tested for permeability coefficient. In the drying process, the samples were dried in the oven at 50°C for 72 h to ensure complete dry. Then, the samples were saturated with the pump-out method by using a superimposed saturator and a vacuum pumping device. The vacuum cylinder was connected to the pump, and the pump was operated for nearly 1 h. Once the pressure gauge reading of the vacuum was similar to the local atmospheric pressure value, water was slowly injected into the vacuum cylinder to enable the samples to be soaked for 48 h and achieve full saturation.

Table 2: Experimental design of this study.

Sample ID	Initial moisture	Curing days	Test items
		1	PT
1	85%	7	PT, UCT, DST
		28	PT, UCT, DST, MIP, SEM, DS (PT, UCT, MIP, SEM)
		1	PT
2	81%	7	PT, UCT, DST
		28	PT, UCT, DST, DS (PT, UCT)
		1	PT
3	77%	7	PT, UCT, DST
		28	PT, UCT, DST, DS (PT, UCT)
		1	PT
4	74%	7	PT, UCT, DST
		28	PT, UCT, DST, MIP, SEM, DS (PT, UCT, MIP, SEM)
		1	PT
5	71%	7	PT, UCT, DST
		28	PT, UCT, DST, DS (PT, UCT)
		1	PT
6	63%	7	PT, UCT, DST
		28	PT, UCT, DST, DS (PT, UCT)
		1	PT
7	56%	7	PT, UCT, DST
		28	PT, UCT, DST, MIP, SEM, DS (PT, UCT, MIP, SEM)

Note: "DS (PT, UCT, MIP, SEM)" above represents conducting tests of PT, UCT, MIP, and SEM on DS samples.

Figure 1: Dewatering equipment of municipal sludge.

2.2.3. *Permeability Test (PT).* The solidified samples with standard curing ages of 1, 7, and 28 d and the DS samples were selected for the PT with deionized water. The permeability test was conducted according to ASTM D5084-03 [25] standards and by using the PN3230M (Geoequip Corporation, USA) flexible wall permeameter. Before the PT, the samples were saturated in a vacuum. During the test, the confining pressure was retained at 100 kPa, the lower osmotic pressure of the samples was 80 kPa, the upper osmotic pressure was 0 kPa, the effective osmotic pressure was 80 kPa, and the room temperature was controlled at 25°C. The scale of the water pipe of the permeameter was recorded every hour. The permeability coefficient of the samples at different times were calculated according to Darcy's law. The relative stable value of permeability coefficient was adopted as the permeability coefficient of the samples.

2.2.4. *Unconfined Compression Test (UCT) and Direct Shear Test (DST).* The solidified sludge samples with different moisture contents cured for 7 and 28 d were selected for the DST and the UCT, according to the standards ASTM D2166 [26] and ASTM D3080 [27] respectively. The UCT was conducted with a universal testing machine. The loading rate was controlled at 2 mm/min. Three parallel experiments were conducted in each group, and the average value was adopted. The error of the parallel samples was less than 5%.

2.2.5. *MIP and SEM Tests.* Samples 1, 4, and 7 (initial moisture contents of 85%, 74%, and 56%), which represent the solidified sludge cured for 28 d before drying-saturated process, were selected for the MIP and SEM tests. During MIP testing, the solidified bodies were broken off carefully. The small sample blocks measuring approximately 1 cm^3 were taken from the fresh section and treated by vacuum freeze-drying technology. The MIP test was conducted by using the PoreMaster-33 (Quantachrome Company, USA) automatic mercury injection.

During SEM testing, the solidified bodies were carefully broken off, and the small test blocks measuring approximately 1 cm^3 were taken from 1 cm from the outer surface of the samples. Then, the broken-off samples were soaked in ethanol at normal temperature for 96 h. Finally, the sample blocks were freeze-dried and evacuated for 12 h. The SEM was conducted with Quanta 250 microscope.

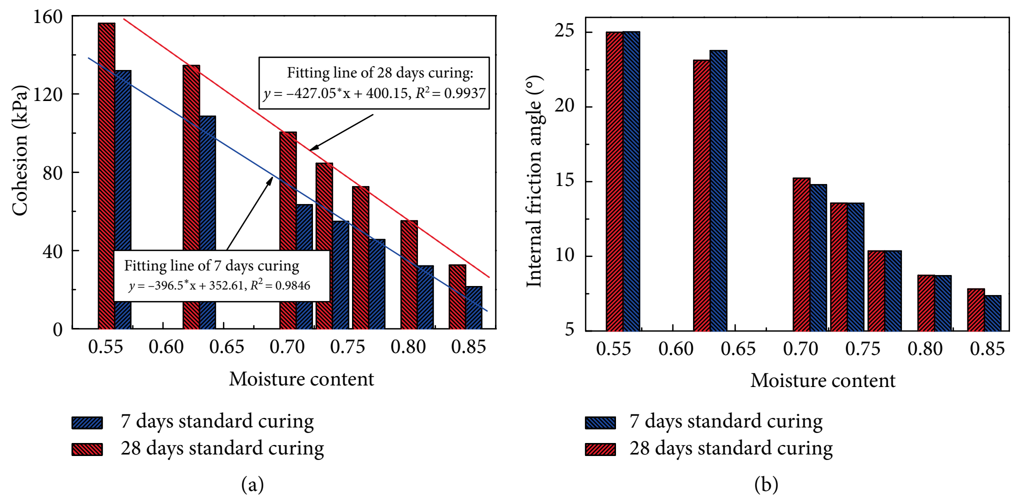

Figure 2: DST results of solidified sludge with different initial moisture contents: (a) cohesion; (b) internal friction angle.

3. Results and Discussion

3.1. Shear Strength and Unconfined Compressive Strength Analysis. The results of the DST of the solidified sludge samples with different initial moisture contents and curing ages of 7 and 28 days are shown in Figure 2. As shown in Figure 2(a), the cohesion of the solidified sludge sample decreases almost linearly as the initial moisture content increases, but is affected inversely by the curing ages. When the curing age increases from 7 days to 28 days, the increasing amplitude of the solidified sludge cohesion ranges from 11 to 37 kPa.

As shown in Figure 2(b), the internal friction angle increases with the decrease in initial moisture content. In particular, the internal friction angle initially increased slowly (moisture content: 85–75%), then increased rapidly (moisture content: 75–60%), and finally increased slowly (moisture content: less than 60%). The internal friction angle of the solidified sludge samples varied minimally with age.

Figure 3 shows the unconfined compressive strength of saturated samples with standard curing for 7 and 28 days. The unconfined compressive strength of the solidified sludge samples increased with the decrease in the initial moisture content of the sludge. The strength of the solidified sludge increased the fastest in the early stage. The increase in the unconfined compressive strength of the samples with standard curing for 28 days was approximately 15% higher than that of the samples cured for 7 days. The unconfined compressive strength of the DS samples with curing for 28 days increased to a certain extent. The main reason may be that the pores of the solidified sludge will largely shrink during the drying process, making the structure denser and then the strength increase. After resaturation, the strength of the solidified body will not decrease due to the good water stability of the solidifying agent.

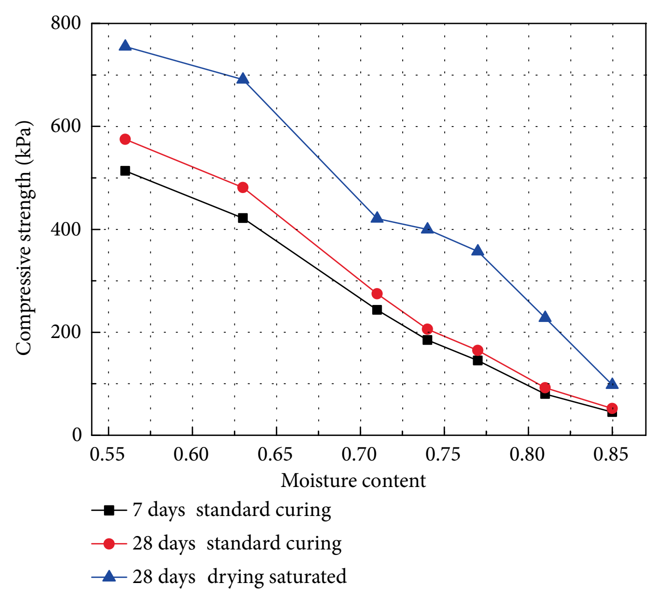

Figure 3: Unconfined compressive strengths of solidified sludge with different initial moisture content.

3.2. Results of the Permeability Test. The changes in the permeability coefficient of the solidified sludge samples with different initial moisture contents and curing ages are shown in Figure 4. Under the modification conditions for 1, 7, and 28 days, all of the permeability coefficient of the solidified sludge samples decreased with the reduction of initial moisture content. The derived values, which were less than 10^{-7} cm/s and all between the magnitude of 10^{-8} and 10^{-10} cm/s, can meet the requirements of permeability coefficient and China's standards for managing the impermeable layers of landfills. The permeability coefficient decreased with the increase of curing age, and the decrease was in 0.5 orders of magnitude.

As shown in Figure 5, the permeability coefficient of the solidified sludge sample with the standard curing for 28 d was the lowest when the initial moisture content was 63%. Then, the permeability coefficient increased significantly for the 28 d of curing after the drying-saturated process. The permeability coefficient of the solidified sludge with different initial contents after the drying-saturated treatment increased in varied extents, and the maximum increase was 4 orders of magnitude. When the initial moisture content of the sludge was 74%, the

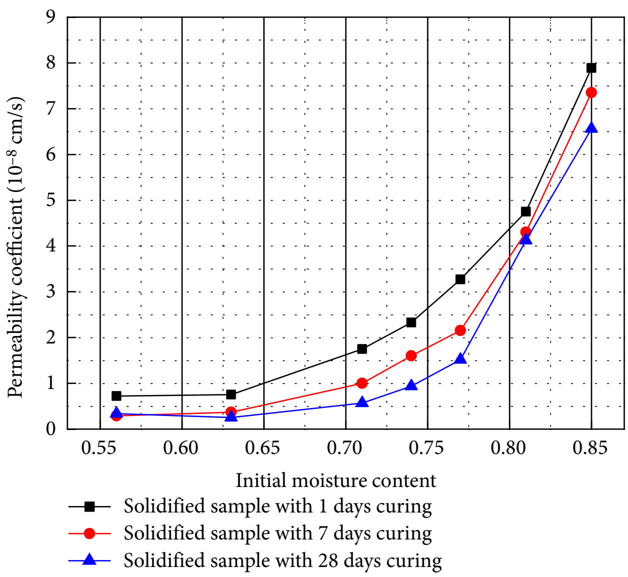

FIGURE 4: Permeability coefficient of solidified sludge with different initial moisture content.

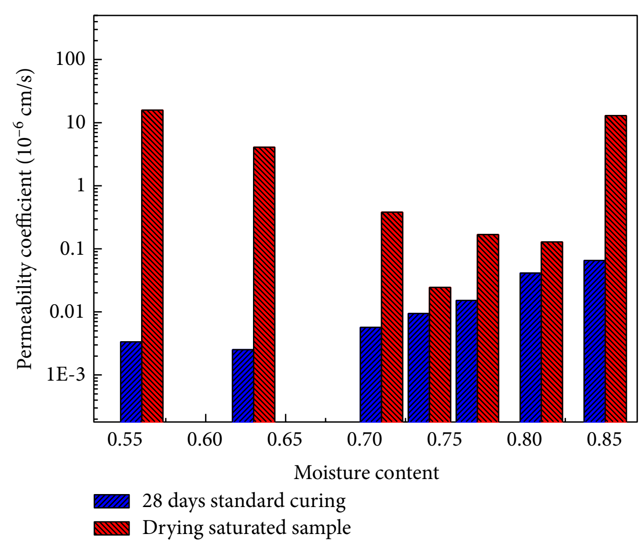

FIGURE 5: Permeability coefficient of solidified sludge body after drying-saturated.

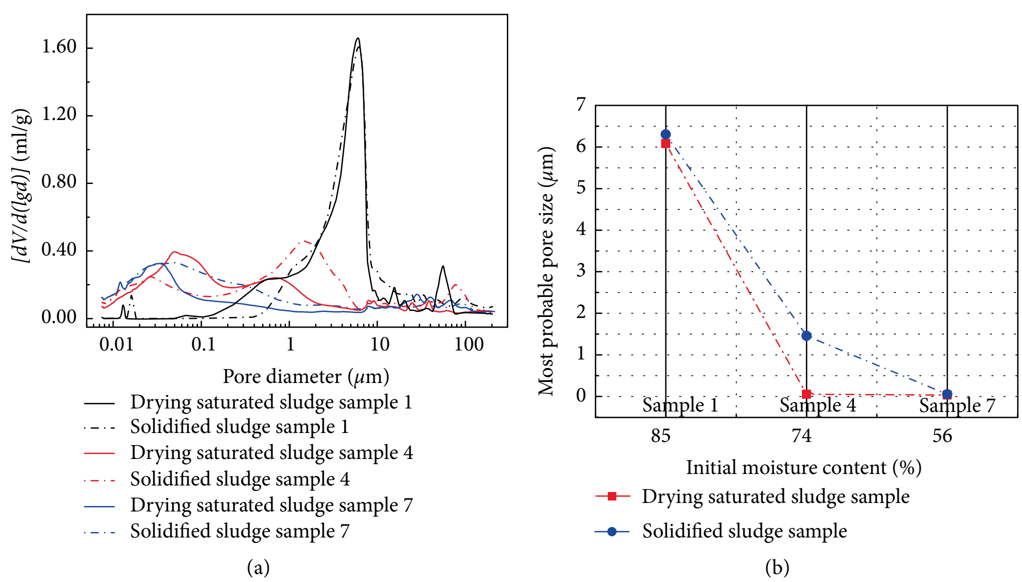

FIGURE 6: MIP results of solidified sludge with different initial moisture contents: (a) pore distribution density; (b) most-probable pore size.

permeability coefficient of the solidified sludge sample after the drying-saturated was the smallest (2.46×10^{-8} cm/s), and the corresponding increase rate was the smallest. This result was consistent with the change of pore diameter in Figure 6.

3.3. Microstructure Analysis of Pores. Microstructure is an important factor for the change of geotechnical properties. The peak value of the differential curve of a pore size distribution is defined as the most-probable pore size. This most-probable pore size definition has a physical meaning, i.e., pores with sizes less than the most-probable pore size cannot easily generate connected pore channels. As shown in Figure 6, the most-probable pore sizes of Samples 1, 4, and 7 (solidified sludge samples) cured for 28 days are 6.30, 1.46, and 0.05 μm, respectively. After the DS process, the corresponding most-probable pore sizes changed to 6.08, 0.05, and 0.04 μm. The pores of the solidified sludge samples were mainly distributed between 0.01 and 200 μm. To facilitate subsequent discussions, the pore sizes were divided into large pores (>100 μm), middle pores (10.0–100.0 μm), small pores (1.0–10.0 μm), mesopores (0.1–1.0 μm), and micropores (<0.1 μm), and all the upper limit were included in the range. The differential pore size distribution, cumulative pore volume, and cumulative pore percentage of the solidified samples with different moisture contents are shown in Figures 6–8.

As shown in Figures 7 and 8, the higher the initial moisture content of the solidified sample, the larger the total pore volume of the solidified sludge will be, that is why the

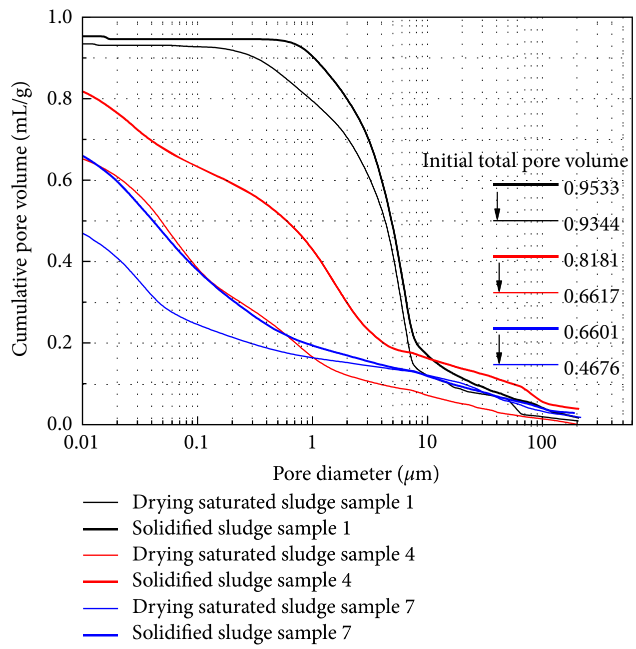

FIGURE 7: Cumulative pore volume of solidified sludge with different initial moisture contents.

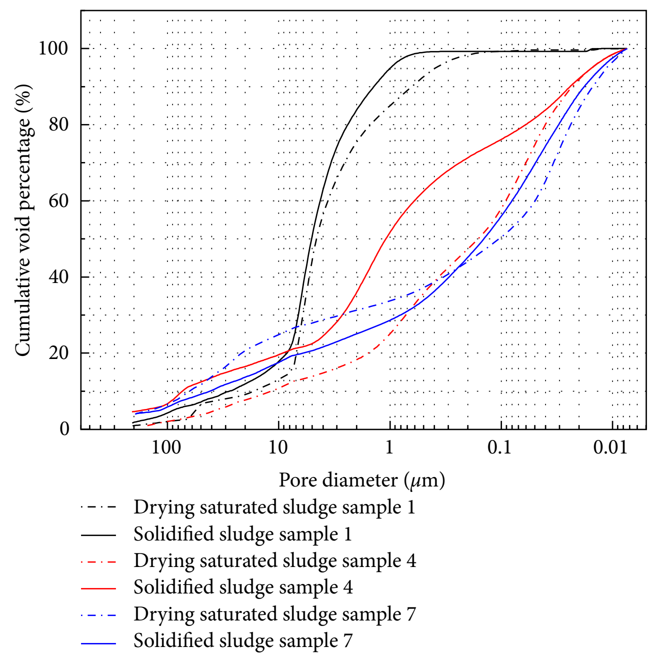

FIGURE 8: Cumulative porosity percentage of solidified sludge with different initial moisture contents.

permeability coefficient decreased with the reduction of initial moisture content. With the decrease of the initial moisture content, the pores transformed from small pores to mesopores and micropores. For example, the total porosity of the solidified sludge (Sample 1) reached 0.953 mL/g when the initial moisture content was 85%. The pores were mainly concentrated as medium and small pores (1.0–10.0 μm), in which the small ones accounted for 80% and the middle ones for 16%. The mesopores was 4% of total porosity, and no micropores were visible. When the initial moisture content was 56% (Sample 7), the total porosity was 0.66 mL/g, and the pores were mainly concentrated in the small pores, mesopores, and micropores (1.0–10.0 μm), accounting for approximately 80% of the total porosity. After drying, the volume of the solidified sludge sample shrunk, thus leading to the reduction of total porosity. Then, the pores moved toward the smaller pore sizes.

Figure 9 presents the varied volumes of the solidified sludge with different moisture contents after drying. The samples shrunk after drying, and the volume shrinkage rate increased initially and then decreased with the decrease in moisture content. When the moisture content was 74%, the volume shrinkage of the sample was the largest at 39.29%.

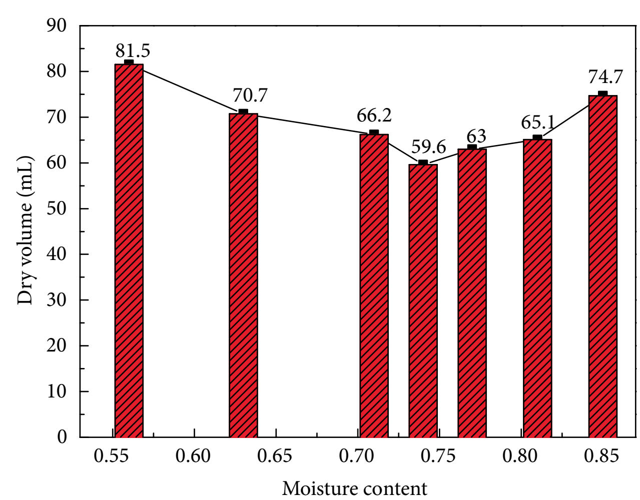

FIGURE 9: Dry volume of solidified sludge with different initial moisture content.

3.4. SEM Image Analysis. The microstructures of the solidified sludge samples with different moisture contents before and after the DS process are shown in Figure 10. Hydrated products were observed in the solidified sludge samples. After DS treatment, the hydrated products of the solidified bodies were distributed relatively more densely. This finding can be attributed to the larger amount of hydration products caused by the volume shrinkage of the dried samples. Moreover, given the variations in the initial moisture contents of the different samples, the contents, forms, and distribution of the hydrated products of the samples also differed from one another. A large number of pores can be seen in the solidified sample (Figure 10(a)) and the DS samples (Figure 10(b)), resulting in poor density. The initial moisture content of Sample 1 was the highest (85%), and the sludge and the solidified bodies were filled with large amounts of water. A substantial number of pores were formed after drying. In addition, the contents of Aft, calcium hydroxide, and other hydrated products in Figure 10(b) were higher than those of Figure 10(a), and the quantities of the solidified bodies composed of sludge particles and reaction products were higher. The difference

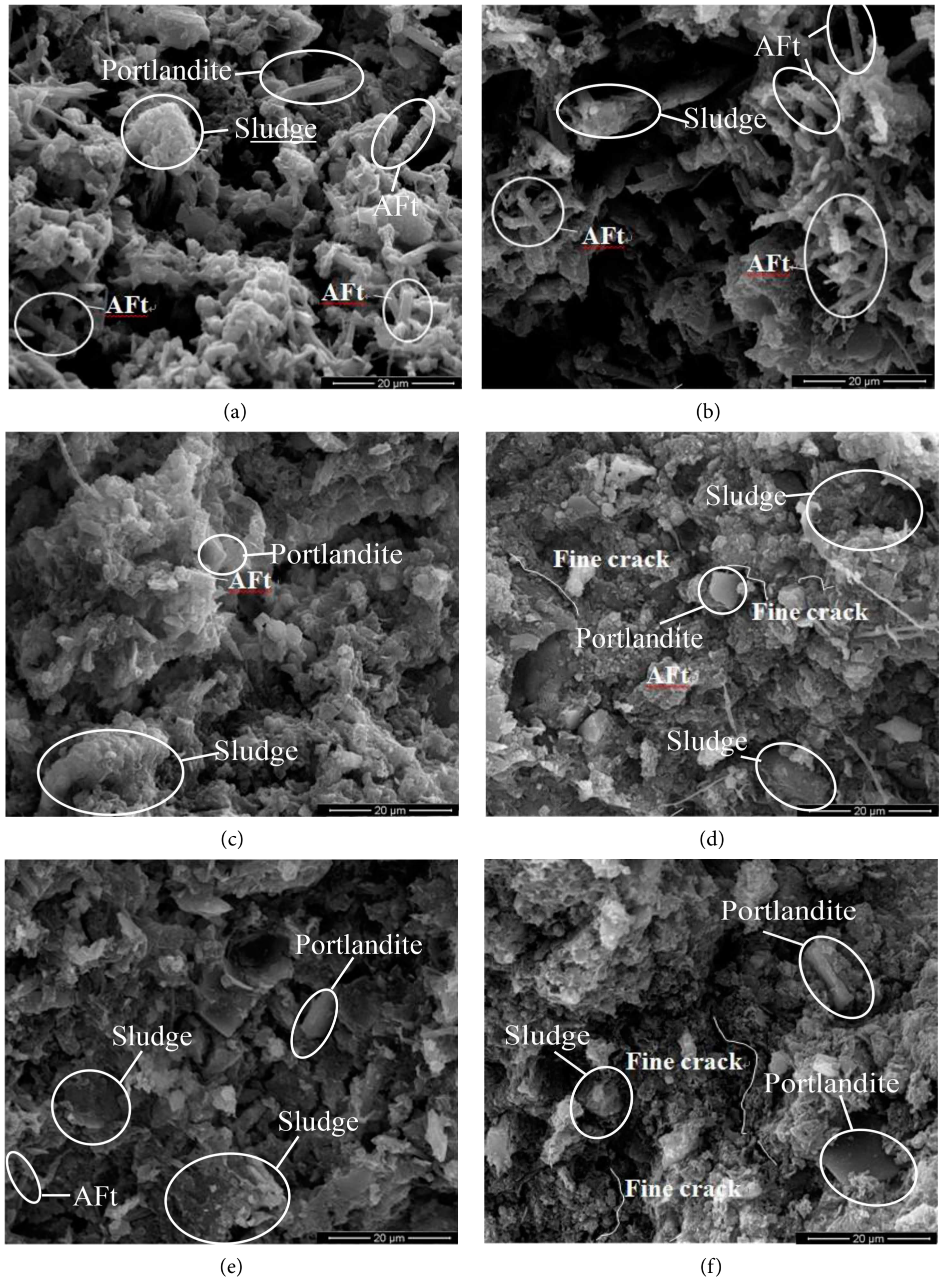

Figure 10: SEM images of solidified sludge bodies under different conditions. (a) Solidified Sample 1. (b) Drying saturated Sample 1. (c) Solidified Sample 4. (d) Drying saturated Sample 4. (e) Solidified Sample 7. (f) Drying saturated Sample 7.

can be explained by volume shrinkage during the drying process. Furthermore, the products became concentrated and subsequently formed additional stents to connect particles and generate connective hydrophobic pores. As a result, the samples after DS treatment had relatively high strengths, and the permeability coefficient markedly increased. The above mentioned findings are consistent with the results of SEM for the solidified sludge samples and the DS samples (Samples 4 and 7). Compared with those of Sample 1, the pores of Samples 4 and 7 were smaller due to their low moisture contents, and thus, microcracks were produced during the drying process. After the DS treatment, the total porosity of the samples decreased but the permeability coefficient increased.

3.5. Discussion. Municipal sewage sludge is currently a major problem in China's urbanization process, and its improper disposal may result in high levels of environmental pollution [28, 29]. Agricultural application, composting, and incineration cannot be widely adopted due to economic or technical reasons, which renders the existing problem of municipal sewage sludge difficult to solve [30, 31]. The application of geotechnical engineering, such as subgrade filling, landfill cover layering, and road base development, to modify municipal sewage sludge provides important ways to solve the sludge disposal problem in China. In geotechnical engineering, the emphasis of the application is solving the geotechnical properties of solidified municipal sewage sludge from different sources and determining the effect of moisture

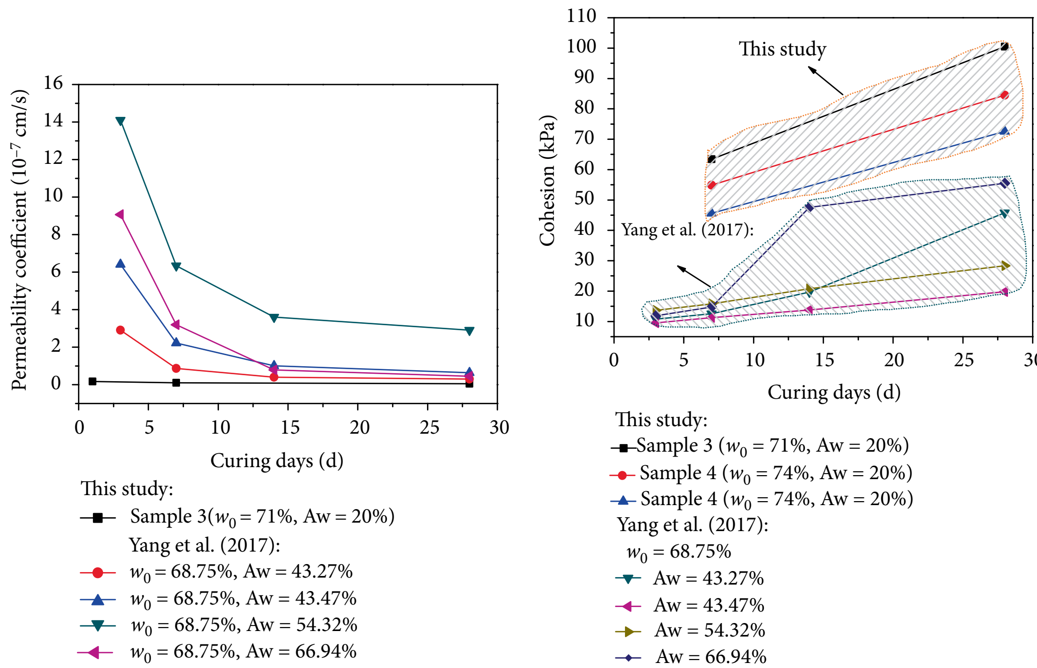

(a) (b)

FIGURE 11: Comparison of geotechnical properties of solidified sludge with Yang et al. [10]: (a) permeability coefficient; (b) cohesion.

content on the geotechnical properties of solidified sludge. Thus, geotechnical engineering technologies can greatly contribute to the disposal of solidified sludge in China.

The results of the test analysis of this study show that the pore distribution of the solidified sludge varies with different moisture contents. The sludge with high moisture content has many pores. Moreover, the contact area between the products of the solidifying agent reaction and the sludge particles is relatively small, and the frictional resistance is also small. With the decrease in moisture content, the total porosity of the solidified sludge sample is reduced. Then, with the increase in contact area between particles, frictional resistance is also increased. Under nondrying condition, the hydrated products produced by cement and other materials in the solidifying agent have filled the pores of the sludge sample. As a result, all of the permeability coefficient of the solidified sludge samples with different moisture contents have decreased with the increase of curing age. At the optimum moisture content, the permeability coefficient of the solidified sludge sample is at the lowest.

The volume of the solidified sludge sample shrinks in the drying process, and the moisture content with the largest shrinkage is 74%. Previous studies [32] showed that when the water-binder ratio is greater than 0.5, the autogenous shrinkage is negligible compared with the drying shrinkage. Therefore, the drying shrinkage of the solidified sludge is mainly determined by the interaction of pore structure, matrix suction, and mechanical properties of the solidified sludge sample. The pore structure determines matrix suction, and the matrix suction and mechanical properties of the solidified sludge sample determine volume shrinkage. The solidified sludge sample formed by the solidified sludge with high initial moisture content has substantial middle and small pores. In the drying process, the matrix suction is small, and the bearing capacity of the pore skeletal structure can effectively resist the matrix suction and thus resist deformation. With the decrease of the initial moisture content, the pore structure of the formed solidified sludge sample changes, and the pores move toward mesopores and micropores. In the drying process, the water losses of the mesopores and micropores lead to the increase in matrix suction. At this time, the ability of the skeletal structure to resist deformation is weakened, and the deformation of the solidified sludge sample increases. When the moisture content decreases at a certain value, the pore structure further changes, the number of mesopores and micropores further increases, the matrix suction in the process of water loss further increases, and the compressive ability of the skeletal structure of the solidified sludge sample increases greatly. The drying shrinkage is reduced relative to the heightened ability to resist deformation.

After the DS treatment, the most-probable pore size of the solidified sludge sample reduces to a certain extent, and the total porosity decreases. The larger the volume shrinkage of the solidified sludge sample is, the greater the decrease in total porosity and the smaller the permeability coefficient will be. However, the permeability coefficient of the solidified sludge sample will eventually increase by orders of magnitude. The findings imply that the huge change in the permeability of the solidified sludge samples is mainly caused by the microcracks produced in the solidified bodies after drying and the altered properties of some organic matters in the sludge during drying, thus leading to the production of highly connective hydrophobic pores. After drying, the volume shrinks to form additional stents to connect the particle, and thus, the structure becomes denser. More importantly, the compression resistance ability of the solidified sludge sample is enhanced greatly, which is an important factor in increasing the compressive strength of the solidified sludge sample.

In order to clarify the better performance of solidifying agent used in this study, the permeability coefficient and cohesion of solidified sludge samples were compared with the results of Yang et al. [10] The solidifying agents used in the study of Yang et al. [10] were composed of one or more materials including ordinary Portland cement, gangue, clay, and fiber, and the initial moisture content of municipal sludge was 68.75%, which is lower than Sample 3 (i.e., 71%) in this study. The addition ratio of solidifying agent by wet sludge in Yang et al. [10] was 43.27%, 43.47%, 54.32%, and 66.94% respectively, which is much larger than the ratio in this study (i.e., 20%). However, as Figure 11(a) shown, the permeability coefficient of Sample 3 in this study was much lower than that in Yang et al. [10], and the cohesion of the solidified sludge samples (Sample 3, 4, and 5) were obviously larger than that of Yang et al. [10] (Figure 11(b)). This indicates that the performance of the solidifying agent in this study is significantly better than that of other compound solidifying agents composed of cement, clay, gangue, etc.

4. Conclusions

The effects of initial moisture content on the geotechnical properties of the solidified sludge were investigated. Typical geotechnical experiments and microscopic tests for the treated sludge were conducted to determine the relationship between initial moisture content variations and the hydraulic and mechanic characteristics of the solidified municipal sludge before and after the drying-saturated treatment. The main conclusions are as follows:

(1) The unconfined compressive strength and the cohesion of the solidified sludge decreased linearly with the increase in moisture content. With the increase in curing ages, the hydration reaction was gradually completed and the cohesion and strength of the samples with different moisture contents increased.

(2) After CERSM modification, the permeability coefficient of the solidified sludge were all below 10^{-7} cm/s. However, after drying-saturated process, the permeability coefficient of solidified sludge can be increased up to 4 times, mainly due to the formation of a considerable number of microconnected pores and microcracks in the process of drying.

(3) Moisture content can remarkably affect the internal pore volume and the pore distribution of the solidified sludge, with the decrease in the initial moisture content, the pores transformed from small pores to mesopores and micropores. Consequently, the altered microstructure influences the engineering properties of the solidified sludge on the applied environment.

Data Availability

The data used to support the findings of this study are included within the article.

Conflicts of Interest

The authors declare that they have no conflicts of interest regarding the publication of this manuscript.

Acknowledgments

This research was supported by the National Science Foundation for Distinguished Young Scholars (51625903), National Natural Science Foundation of China/Hong Kong Research Grants Council Joint Research Scheme under grant (51861165104), National Natural Science Foundation of China (51609241), Youth Innovation Promotion Association CAS (2017376).

References

[1] Q. Xue and Y. J. Chen, "Study on dewaterability of municipal sludge conditioning by physical conditioners with ultrasonic and magnetic field application," *Desalination and Water Treatment*, vol. 52, no. 34–36, pp. 6396–6402, 2014.

[2] M. Kacprzak, E. Neczaj, K. Fijałkowski et al., "Sewage sludge disposal strategies for sustainable development," *Environmental Research*, vol. 156, pp. 39–46, 2017.

[3] F. Macías, R. Pérez-López, M. A. Caraballo, C. R. Cánovas, and J. M. Nieto, "Management strategies and valorization for waste sludge from active treatment of extremely metal-polluted acid mine drainage: a contribution for sustainable mining," *Journal of Cleaner Production*, vol. 141, pp. 1057–1066, 2017.

[4] R. de Medeiros Paulino, C. M. L. Costa, and Y. D. J. Costa, "Geotechnical study on the use of sanitized sewage sludge in cover layers of solid waste landfills," *Applied Mechanics and Materials*, vol. 872, pp. 143–148, 2017.

[5] S. Oh and W. S. Shin, "Applicability of solidified/stabilized dye sludge char as a landfill cover material," *KSCE Journal of Civil Engineering*, vol. 21, no. 7, pp. 2573–2583, 2017.

[6] D. F. Lin, H. L. Luo, D.-H. Hsiao, C.-T. Chen, and M. Cai, "Enhancing soft subgrade soil with a sewage sludge ash/cement mixture and nano-silicon dioxide," *Environmental Earth Sciences*, vol. 75, no. 7, p. 619, 2016.

[7] S. S. Chu, D. M. Wu, L. L. Liang et al., "Municipal sewage sludge compost promotes Mangifera persiciforma tree growth with no risk of heavy metal contamination of soil," *Scientific Reports*, vol. 7, no. 1, Article ID 13408, 2017.

[8] M. A. I. Juel, A. Mizan, and T. Ahmed, "Sustainable use of tannery sludge in brick manufacturing in Bangladesh," *Waste Management*, vol. 60, pp. 259–269, 2017.

[9] G. Yang, G. M. Zhang, and H. C. Wang, "Current state of sludge production, management, treatment and disposal in China," *Water Research*, vol. 78, pp. 60–73, 2015.

[10] J. K. Yang, H. J. Lu, X. Zhang, J. X. Li, and W. W. Wang, "An experimental study on solidifying municipal sewage sludge through skeleton building using cement and coal gangue," *Advances in Materials Science and Engineering*, vol. 2017, Article ID 5069581, 13 pages, 2017.

[11] C. M. Vu, T. A. Le, T. Satomi, and H. Takahashi, "Study on effect of chemical composition of geopolymer to improve sludge by using fiber materials," *Advanced Experimental Mechanics*, vol. 2, pp. 168–173, 2017.

[12] M. Boutouil and D. Levacher, "Effect of high initial water content on cement-based sludge solidification," *Proceedings of the Institution of Civil Engineers—Ground Improvement*, vol. 9, no. 4, pp. 169–174, 2005.

[13] C. Hsieh, J.-H. Wu, and X.-J. Lu, "Electro-kinetic techniques and geotextiles for high water content sludge dehydration tests," *Japanese Geotechnical Society Special Publication*, vol. 2, no. 65, pp. 2221–2225, 2016.

[14] Y. Feng, X. Y. Luo, and W. A. Lin, "Study on the engineering characteristics of sludge disposal in the repository," *Rock and Soil Mechanics*, vol. 1, pp. 115–122, 2013.

[15] Y. Wan, Q. Xue, and Y. J. Chen, "Construction and application of a unified analytical model for the stability of landfill cover system," *Rock and Soil Mechanics*, vol. 34, no. 6, pp. 1636–1644, 2013.

[16] J. Y. Shi and J. Wang, "Mechanical behavior test study of sludge mixed with municipal solid waste," *Rock and Soil Mechanics*, vol. 33, no. 11, pp. 3208–3212, 2012.

[17] X. T. Hu, B. Liang, and Y. J. Chen, "Study of the influence of freezing and thawing on strength and deformation properties of solidified sewage sludge," *Journal of Experimental Mechanics*, vol. 4, pp. 557–563, 2016.

[18] L. Y. Feng, J. Y. Luo, and Y. G. Chen, "Dilemma of sewage sludge treatment and disposal in China," *Environmental Science & Technology*, vol. 49, no. 8, pp. 4781–4782, 2015.

[19] A. Mahmoud, A. F. A. Hoadley, J.-B. Conrardy, J. Olivier, and J. Vaxelaire, "Influence of process operating parameters on dryness level and energy saving during wastewater sludge electro-dewatering," *Water Research*, vol. 103, pp. 109–123, 2016.

[20] C. Lin, W. Zhu, and J. Han, "Geotechnical properties of solidified sludge by mixing cement and calcium-bentonite," in *Contemporary Topics in Ground Modification, Problem Soils, and Geo-Support*, pp. 281–288, ASCE, 2009.

[21] S. Horpibulsuk, N. Miura, and T. S. Nagaraj, "Clay-water⁄cement ratio identity for cement admixed soft clays," *Journal of Geotechnical and Geoenvironmental Engineering*, vol. 131, no. 2, pp. 187–192, 2005.

[22] Z. Wang, S. F. Xu, L. L. Yan, P. Guo, and Q. Chen, "Shrinkage properties of cement solidified sludge with high water content," *Advanced Materials Research*, pp. 1496–1500, vol. 168, Trans Tech Publications, 2011.

[23] Y. J. Chen, "Engineering characteristics and regulation mechanism of ecological sludge evapotranspiration cover slopes for landfill closure," The University of Chinese Academy of Sciences, 2015.

[24] X. T. Hu, B. Liang, and Y. J. Chen, "Different particle size effects on slag waste incineration characteristics of municipal sewage sludge solidification Engineering," *Chinese Journal of Environmental Engineering*, vol. 11, pp. 5567–5572, 2015.

[25] ASTM D5084-03, *Standard Test Methods for Measurement of Hydraulic Conductivity of Saturated Porous Materials using a Flexible Wall Permeameter*, ASTM International, West Conshohocken, PA, 2003.

[26] ASTM D2166/D2166M-16, *Standard Test Method for Unconfined Compressive Strength of Cohesive Soil*, ASTM International, West Conshohocken, PA, 2016, http://www.astm.org.

[27] ASTM D3080/D3080M-11, *Standard Test Method for Direct Shear Test of Soils under Consolidated Drained Conditions*, ASTM International, West Conshohocken, PA, 2011, http://www.astm.org.

[28] T. V. Rakotonimaro, C. M. Neculita, B. Bussière, M. Benzaazoua, and G. J. Zagury, "Recovery and reuse of sludge from active and passive treatment of mine drainage-impacted waters: a review," *Environmental Science and Pollution Research*, vol. 24, no. 1, pp. 73–91, 2017.

[29] T. P. Thomsen, Z. Sárossy, J. Ahrenfeldt, U. B. Henriksen, F. J. Frandsen, and D. S. Müller-Stöver, "Changes imposed by pyrolysis, thermal gasification and incineration on composition and phosphorus fertilizer quality of municipal sewage sludge," *Journal of Environmental Management*, vol. 198, pp. 308–318, 2017.

[30] P. Devi and A. K. Saroha, "Utilization of sludge based adsorbents for the removal of various pollutants: a review," *Science of the Total Environment*, vol. 578, pp. 16–33, 2017.

[31] M. Y. Xing, C. R. Li, and L. Xiang, "Influence of agricultural utilization of sewage sludge vermicompost on plant growth," *International Journal of Environmental and Ecological Engineering*, 2017.

[32] Y. L. Guo, *Study on Autogenous Shrinkage of Cement Based Cementitious Materials*, Beijing University of Technology, 2006.